Journal of Materials and Environmental Sciences
ISSN : 2028-2508
CODEN : JMESCN

JMES, 2017 Volume 8, Issue 11, Page 3943-3952

http://www.jmaterenvironsci.com /

Experimental and theoretical investigation of 3-methyl-1,2,4-triazole-5-thione derivatives as inhibitors for mild steel corrosion in acid medium

B. Ait Haddou[1], D. Chebabe[2], A. El Assyry[3]*, A. Dermaj[1], M. Touil[4], S. Ibn Ahmed[1], N. Hajjaji[1]

[1]*Laboratory of Materials, Electrochemistry and Environment, FS, University Ibn Tofail, B.P 133, 1400, Kenitra, Morocco*
[2]*Laboratory of Natural Substances & Synthesis and Molecular Dynamic, Faculty of Sciences and Techniques, University of Moulay Ismail, BP 509, Boutalamine, 52000 Errachidia, Morocco*
[3]*Laboratory of Optoelectronic, Physical Chemistry of Materials and Environment, Department of Physics, FS, Ibn Tofail University, PB 133, 1400 Kenitra, Morocco.*
[4]*Chemistry Dept., ESCTM, Ibn Tofail University, P.O. Box 133, Kenitra 14000, Morocco*

Received 24 Jun 2016,
Revised 22 May 2017,
Accepted 24 May 2017

Keywords
- ✓ Triazole surfactants derivatives,
- ✓ Steel,
- ✓ Corrosion inhibitors,
- ✓ Adsorption,
- ✓ DFT.

abdeslam_elassyry@yahoo.fr ;
Phone: +212662662468;

Abstract

The corrosion inhibition of mild steel in HCl acid solutions by some new triazole surfactants derivatives namely 2-(5- decylthio-3-methyl-1,2,4-triazole)acetic acid (MTSC10AC), 2-(5-undecylthio-3-methyl-1,2,4-triazole) acetic acid (MTSC11AC), 2-(5-dodecylthio-3-methyl-1,2,4-triazole) acetic acid (MTSC12AC) have been studied using electrochemical polarization method and electrochemical impedance spectroscopy measurements. These inhibitors have also been studied computationally using density functional theory (DFT). Observable correlation was found between corrosion inhibition efficiency and quantum chemical parameters, using the linear quantitative structure–activity relationship (QSAR) models.

1. Introduction

The study of corrosion inhibition is a very active field of research; several classes of organic compounds are widely used as corrosion inhibitors for metals in acid environments [1-8]. Numerous studies on corrosion inhibition using triazole derivatives as steel corrosion inhibitors have been reported [9, 10]. It has been accepted that the corrosion inhibition process results from the formation of organic inhibitor films on the metal surface.
Experimental means are useful to explain the inhibition mechanism but they are often expensive and time-consuming. Ordinary steel is widely used in various industrial operations, especially, in petroleum industries and power plants [11]. These industries occurs in environments in which, acids are widely used for pickling, cleaning acid, acidification of oil wells and other applications, allowing acid corrosion to take place. The experimental inhibitive properties of three different organic compounds, 2-(5-decylthio-3-methyl-1,2,4-triazole) acetic acid (MTSC10AC), 2-(5-undecylthio-3-methyl-1,2,4-triazole) acetic acid (MTSC11AC) and 2-(5-dodecylthio-3-methyl-1,2,4-triazole) acetic acid (MTSC12AC) have been reported by our group. The quantum chemical calculations were performed at the DFT level using Becke's three-parameter functional in combination with the Lee–Yang–Parr correlation functional (B3LYP) [12]. The calculations were carried out using the Gaussian 09 program [13]. The spherical 6-31G+(d,p) basis sets were used. Calculated molecular properties, comprising the energy of the highest occupied molecular orbital (HOMO), the energy of the lowest unoccupied molecular orbital (LUMO), LUMO- HOMO energy gap (ΔE), dipole moment (μ), the total negatives charges (TNC), molecular volume (V_i), and the polarizability **<α>,** have been correlated to experimental results.

Quantitative structure–activity relationship (QSAR) analysis [14] has been used to correlate the corrosion inhibition activity of the studied molecules with the molecular structures.

2. Methods

2.1. Synthesis

3-methyl-1,2,4-Triazole-5-thione is not commercially available so we prepared it by using a new method in our laboratory using two steps: (1) The synthesis of the 1-acetylthiosemicarbazide by heating thiosemicarbazide and acetic acid during 4 hr. (2) The intramolecular cyclization in ethanol and in the presence of sodium leads to the formation of the MTS in 80%. (Scheme 1)

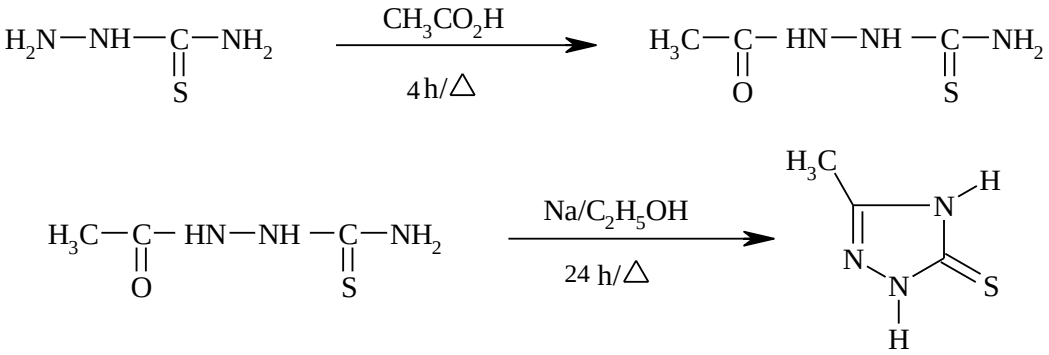

Scheme 1: Synthetic route of 1-acetylthiosemicarbazide and 3-methyl-1,2,4-triazole-5-thione

The synthesis of monopolar surfactants type 5-alkylthio-3-methyl-1,2,4-triazole (MTSCn) were obtained by reacting the 3-methyl-1,2,4-Triazole-5-thione with some alkyl bromide using PTC method, which gave isolated monopolar surfactants (MTSCn (n=9, 10, 11). (Scheme 2)

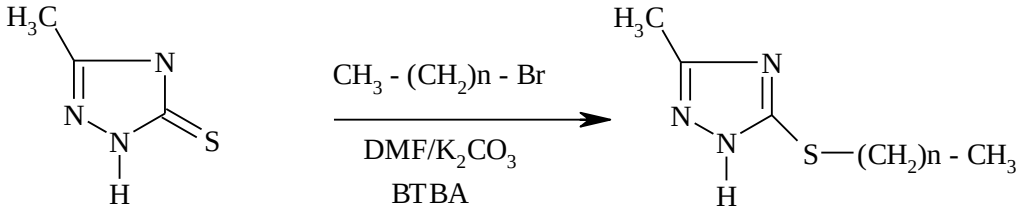

Scheme 2: Synthetic route of 5-alkylthio-3-methyl-1,2,4-triazole

The obtained products have been purified and characterized by ^{1}H NMR, and ^{13}C NMR spectra [15]. To investigate chemical behavior of compounds 5-alkylthio-3-methyl-1,2,4-triazole, they were reacted with bromoacetic acid in ethanol in the presence of Na_2CO_3. The examination of the ^{1}H NMR and ^{13}C NMR spectra of the products showed formation of the monopolar surfactants derived from 2-(5- alkylthio-3-methyl-1,2,4-triazole)acetic acid MTSCnAc (n=9, 10, 11) (Scheme 3)

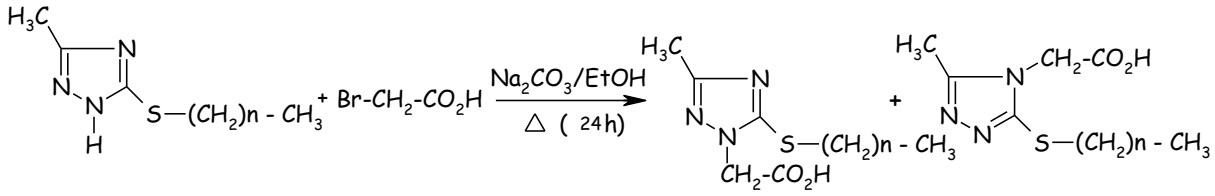

Scheme 3: Synthetic route of 2-(5- alkylthio-3-methyl-1,2,4-triazole)acetic acid

These products were obtained with a yield close to 80% and characterized by ^{1}H NMR and ^{13}C NMR.

Spectral characteristics:

n= 9: MTSC10AC. ^{1}H NMR (300MHZ, DMSOd6/TMS) : 1.1-1.9 ppm (m,42H, $2(CH_2)_9$-CH3); 2.5 ppm (s, 3H, CH_3); 2.46 ppm (s, 3H, CH_3), 3.2(t,2H, $CH_2\alpha S$), 3.25(t,2H, $CH_2\alpha S$), 4.71 ppm (s, 2H, $CH_2\alpha C{=}O$), 4.66 ppm (s, 2H, $CH_2\alpha C{=}O$).

MTSC10AC. ^{13}C NMR (50MHZ, DMSOd6/TMS)

* Chaîne alkyle :11.91, 22.81, 29.15, 29.43 , 29.87, 32.07, 32.15.
* 1,2,4-triazole:13.84 et 14.10 ($2CH_3$); 153.29 et 154.74 (2C3); 158.77 et 160.76 (2 C5)
* Deux C=O : 173.36 et 173.64 ppm.
* Les CH_2 en α du C=O: 50.80 et 51.48 ppm.

n= 10: MTSC11AC, ^1H NMR (300MHZ, DMSOd6/TMS) 0.87-1.61 ppm (m,46H, 2(CH2)10-CH3); 2.30 ppm (s, 3H, CH3); 2.24 ppm (s, 3H, CH3), 2.98(t,2H, CH_2αS), 3.09(t,2H, CH_2αS), 4.52 ppm (s, 2H, CH_2αC=O), 4.57 ppm (s, 2H, CH_2αC=O).

MTSC11AC, ^{13}C NMR (50MHZ, DMSOd6/TMS)

* Chaîne alkyle :11.91, 22.81, 29.15, 29.43, 29.55, 29.87, 32.07, 32.15.
* 1,2,4-triazole:13.84 et 14.10 (2CH3); 153.29 et 154.74 (2C3); 158.77 et 160.76 (2 C5)
* Deux C=O : 173.36 et 173.64 ppm.
* Les CH_2 en α du C=O: 50.86 et 51.43 ppm.

n= 11: MTSC12AC, ^1H NMR (300MHZ, DMSOd6/TMS) 1.04 -1.8 ppm (m, 50H, 2(CH2)11-CH3); 2.43 ppm (s, 3H, CH3); 2.50 ppm (s, 3H, CH3), 3.17(t, 2H, CH2αS), 3.26(t,2H, CH2αS), 4.72 ppm (s, 2H, CH2αC=O), 4.77 ppm (s, 2H, CH2αC=O).

MTSC12AC, ^{13}C NMR (50MHZ, DMSOd6/TMS)

* Chaîne alkyle : 11.88, 22.78, 29.09, 29.41, 29.51, 29.83, 29.89, 32.04, 33.43.
* 1,2,4-triazole:13.80 et 14.08 ($2CH_3$); 153.16 et 154.74 (2C3); 158.45 et 160.56 (2 C5).
* Deux C=O: 173.09 et 173.4 ppm.
* Les CH_2 en α du C=O : 51.73 et 52 ppm.

2.2. Computational details

The aim of this theoretical study is to investigate structural relationships between the corrosion-inhibition efficiency and molecular properties of the (MTSC10AC), (MTSC11AC) and (MTSC12AC) molecules calculated at the density functional theory (DFT) level. These molecular properties are mainly the energies of the highest occupied molecular orbital (HOMO), the energy of the lowest unoccupied molecular orbital (LUMO), LUMO- HOMO energy gap (ΔE), dipole moment (μ), the total negatives charges (TNC), molecular volume (V_i), and the polarizability <α>. Solvent effects were accounted for by using the polarizable continuum model (PCM) [16] using self-consistent reaction field approach with the dielectric constant equal to 78.39. The calculations were extended to the protonated forms of the molecules under study.

3. Results and Discussion

3.1. Experimental results

Inhibition of corrosion of mild steel by using the substituted Triazole derivatives as corrosion inhibitors was investigated experimentally [17]. Table 1 summarizes the impedance and electrochemical parameters of corrosion of mild steel in 1M HCl solution by different concentrations of MTSC10AC, MTSC11AC and MTSC12AC.

Table 1. Impedance and electrochemical parameters of corrosion of mild steel in 1M HCl solution by different concentrations of MTSC10AC, MTSC11AC and MTSC12AC.

Inhibitors	C (M)	Re (ohm.cm^2)	Rf (ohm.cm^2)	Cf (μF/cm^2)	Rt (ohm.cm^2)	Cd (mF/cm^2)	E%	E_{corr} (mv)	I_{corr} (μA)	βa (mv)	E%
	0	2.07	----	----	8.2	2.63	----	-487	393	86	----
MTSC10AC	10^{-5}	2.2	0.054	80	67	1.13	86	-482	69	35	82
	10^{-4}	2.34	0.012	22	78	1.14	88	-479	68	31	83
	510^{-4}	3.3	1.60	18	152	0.82	93	-465	38	34	90
	10^{-3}	2.00	0.0024	9.57	170	0.80	94	-484	34	36	91
MTSC11AC	10^{-5}	1.41	0.79	38	76	0.33	89	-466	87	23	78
	10^{-4}	1.46	0.98	15	131	0.24	93	-444	47	38	88
	510^{-4}	1.85	1.15	14	148	0.06	93	-485	36	33	91
	10^{-3}	1.82	1.8	8.9	212	0.54	96	-462	38	43	90
MTSC12AC	10^{-5}	1.14	0.93	27	110	0.88	91	-487	82	46	79
	10^{-4}	1.20	4.31	12	114	0.51	93	-485	34	30	91
	510^{-4}	1.38	0.90	8.9	224	0.55	96	-484	29	29	93
	10^{-3}	1.65	0.40	11	130	0 .96	94	-440	35	28	91

Table 1 clearly indicates that the rate of corrosion decreased in the presence of MTSC10AC, MTSC11AC and MTSC12AC. This effect is very marked at the highest concentrations of the inhibitors, *E*% increases with inhibitor concentration, reaching 86 % for MTSC10AC, 87 % for MTSC11AC and 92 % for MTSC12AC at 10^{-5} M. All three compounds inhibited corrosion of steel in 1M HCl, with MTSC12AC being the best inhibitor. Classification of these inhibitors according to efficiency is: MTSC12AC >MTSC11AC >MTSC10AC. Examination of Table 1 shows that Since MTSC12AC in low concentration has given a better efficiency (92%, 93%, 96% and 94%) than other compounds; thus, MTSC12AC is the best inhibitor.

By comparison with studies previously carried out in our laboratory using 5-alkylthio-3-methyl-1,2,4-triazole (MTSCn) [10], it can be concluded that the grafting of the carboxylic acid function significantly increases the inhibition efficiency. Thus, it goes from 92% for MTSC12AC to 72% for MTSC12.

3.2. Quantum chemical study of neutral inhibitors

In order to understand the experimental results, the neutral inhibitors forms of the surfactant molecules were studied computationally and the quantum chemical parameters most relevant to their potential action as corrosion inhibitors have been calculated in gas phase and in aqueous phase with B3LYP using 6-31G+(d,p) basis sets. E_{HOMO} is often associated with the electron donating ability of the molecule and inhibition efficiency increases with increasing E_{HOMO} values. High E_{HOMO} values indicate that the molecule has a tendency to donate electrons to appropriate acceptor molecules with low energy empty molecular orbital [18, 19]. Increasing values of the E_{HOMO} facilitate adsorption (and therefore inhibition) by influencing the transport process through the adsorbed layer. On the other hand, E_{LUMO} indicates the ability of accepting electrons to molecule. The lower the value of E_{LUMO}, the more probable, it is that the molecule would accept electrons [20].This fact proves that the feedback bonds are formed between d-orbitals of steel and inhibitor molecules. Forming of feedback bonds increases the chemical adsorption of inhibitor molecules on the steel surface [18, 21], and so increases the inhibition efficiency. The energy gap (ΔE) between the HOMO and LUMO energy levels of an inhibitor is another parameter that can be used to predict the extent of corrosion inhibition. The larger values of the energy gap implies high stability for the molecule in chemical reactions [22], and the smaller values indicates that the molecule is the more probable to give higher inhibition efficiency.

3.2.1. In gas phase

The quantum chemical parameters of the neutral molecules in gas phase are given in Table 2. From the Table, it might be considered that there is no simple correlation between inhibitor properties and the energies of the frontier orbitals (E_{HOMO} and E_{LUMO}), because all studied molecules with different corrosion inhibitor properties gives approximately the same E_{HOMO}, E_{LUMO} and (ΔE).

Table 2. The calculated quantum chemical parameters for MTSC10AC, MTSC11AC and MTSC12AC in the neutral form obtained using DFT at the B3LYP/6-31+G (d, p) basis set in gas phase.

Molecule	E_{HOMO} (eV)	E_{LUMO} (eV)	ΔE (eV)	μ (Debye)	TNC	Vi (cm3/mol)	<α> (ua)
MTSC10AC	-6.6597	-1.9744	4.6853	2.6120	-8.498	275.096	228.01
MTSC11AC	-6.6586	-1.9736	4.6850	2.6452	-8.957	265.605	239.85
MTSC12AC	-6.6576	-1.9728	4.6848	2.6124	**-9.416**	**335.372**	**251.68**

On the other hand, dipole moment (μ), the total negatives charges (TNC), molecular volume (V_i), and the polarizability <α> were calculated in gas phase and in aqueous phase, for more information on the reactivity of molecules under study. These parameters are closely responsible for the physical adsorption. This last, results from electrostatic interaction between the charged centers of molecules and charged metal surface which results in a dipole interaction of molecules and metal surface. Dipole moment is the measure of the asymmetry in the molecular charge distribution and the polarity of a polar covalent bond. It is defined as the product of charge on the atoms and the distance between the two bonded atoms [23]. It is mainly used to study the intermolecular interactions involving the Van der Waals type dipole–dipole forces, because the larger the dipole moment the stronger will be the intermolecular attraction [24], thus, the high value of dipole moment probably increases the adsorption between chemical compound and metal surface [25]. Another way of obtaining information about the distribution of electrons is made by computing polarizability depending on the second derivative of the energy with respect to electric field, which is defined as follows:

$$\alpha = \left(\frac{\partial^2 E}{\partial F_a \partial F_b} \right) \qquad a, b = x, y, z$$

The mean value of the polarizability is evaluated by following:

$$<\alpha>=\frac{1}{3}\left(\alpha_{xx}+\alpha_{yy}+\alpha_{zz}\right)$$

The minimum polarizability principle (MPP) has been postulated [26], which expects that the natural direction of evolution of any system be towards a state of minimum polarizability. The most stable species (reactants or products) have the lowest sum of <α> in chemical reactions [27, 28], inversely, the most reactive species are those that have a high polarizability. The inhibition efficiency increases as the volume (V_i) of the molecules increases due to the increase of the contact area between molecule and surface. The highest molecular volume leading to increase both of its adsorptive properties on the metal surface and inhibition efficiency [29]. The accumulated distribution of negative charges (TNC) is another important factor that should be considered, the more negative charges that are accumulated at the adsorption centres, the more electrostatic interaction between them and charged metal surface, therefore, the more readily the electron is donated to the unoccupied orbital of the surface atom of the metal [30]. Table 1 show that there is no simple relation or direct trend relationship can be derived with the inhibition performance of this class of neutral inhibitors and dipole moment. However, (MTSC12AC) has the highest value of the mean polarizability (251.68 ua), which probably increases it reactivity and increases the inhibition efficiency. It is clear from our results that (MTSC12AC) presents the highest molecular volume V_i (335.372 cm^3/mol), which increases contact area, thereby increasing it adsorption on the metal surface, and has also more negative charges TNC (-9,416 e),leading to a strong electrostatic interaction between the adsorption centres and charged metal surface. This result leads us to propose that interaction between this class of neutral inhibitors and metal surface of steel is electrostatic (physisorption).

3.2.2. In aqueous phase

The phenomenon of electrochemical corrosion in acidic medium occurs in the liquid phase, and it is well known that the inhibitory molecules in solution act otherwise than in a vacuum, this is why, it is relevant to include the effect of solvent in the computations. The solvent effect on molecular structure of solute could be studied by a model, which is known as polarized continuum model (PCM) [16]. The Polarizable Continuum Model (PCM) [31, 32] is one of the most successful models, thanks to its generality and its versatility. The PCM represents a solvent, or other more complex matrices [33] such as an anisotropic medium or a weak ionic solution or even a metal nanoparticle, by means of a polarizable, infinite, dielectric medium which surrounds a molecular cavity that accommodates the "solute". In this paper, we have chosen the CPCM polarizable conductor calculation model implemented inGaussian09 program. All geometries of the molecules involved are optimized at DFT levels with B3LYP functional using 6-31+G(d, p) basis set and the calculated quantum chemical parameters in the aqueous phase are summarized in Table 3. It is clear that the calculated quantum chemical parameters in the presence of a solvent (water) differ significantly from those calculated in the gas phase. In fact, a significant decrease is shown for E_{HOMO} (-6.8902 vs. -6.6576 eV) and inversely, a considerable increase is shown for E_{LUMO} (-1.0449 vs. -1.9728 eV) for (MTSC12AC). this result is normal, because all nucleophiles will be less reactive in protic (water) than aprotic solvents, what derives from the stabilization of the frontier molecular orbitals (FMO) through one or all of the various non-covalent interactions with the solvent such as H-bonding, dipole-dipole interactions, Van der Waals interactions. It is shown also from the Table 3 that a considerable increase for μ (3.9683 vs. 2.6124 Debye), TNC (-9.5628 vs. -9,416 e) and <α> (327.08 vs. 251.68 ua) for (MTSC12AC). Therefore, we can expect a considerable increase in the electrostatic interaction between the active sites on inhibitors and the iron metal surface compared to the previous cases; which facilitates physical adsorption.

Table 3. The calculated quantum chemical parameters for MTSC10AC, MTSC11AC and MTSC12AC in the neutral form obtained using DFT at the B3LYP/6-31+G (d, p) basis set in aqueous phase.

Molecule	E_{HOMO} (eV)	E_{LUMO} (eV)	ΔE (eV)	μ (Debye)	TNC (e)	Vi (cm3/mol)	<α> (ua)
MTSC10AC	-6.8897	-1.0427	5.8470	3.9650	-8.6413	264.780	297.62
MTSC11AC	-6.8908	-1.0454	5.8454	4.0177	-9.1018	312.265	312.30
MTSC12AC	-6.8902	-1.0449	5.8453	3.9683	-9.5628	272.024	327.08

In a general way, our results about the frontier orbitals does not allow us to draw a clear correlation between these orbitals and the inhibitory potency of these molecules, which led us to make other calculations taking into account the effect of protonation. The contour plots of the Kohn–Sham HOMO and LUMO are shown in Fig. 2, from the figures, it may be considered that (MTSC10AC), (MTSC11AC) and (MTSC12AC) have similar

HOMO and LUMO frontier orbitals electron density distributions, which are all located practically on the hydrophilic fragments of surfactant molecules, and are mainly localized on the nitrogen atoms (N) and on the sulfur atom (S) indicating that are the preferred sites for the electrophilic attack.

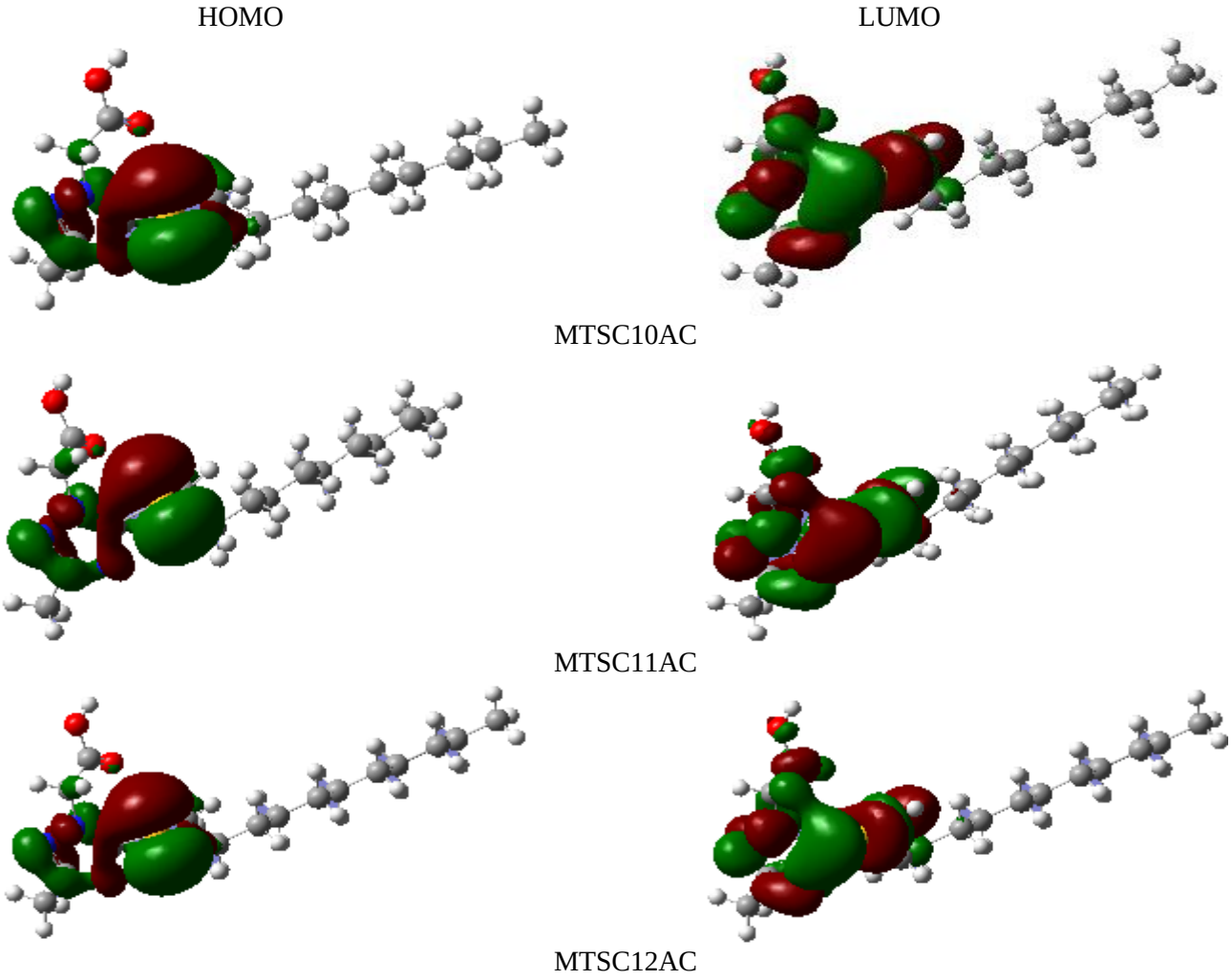

Fig.2. Contour plots of the Kohn–Sham of HOMO and LUMO of the (MTSC10AC, MTSC11AC and MTSC12AC) as obtained at the B3LYP/6-31+G(d, p) level in the neutral form.

3.3. Quantum chemical study of protonated inhibitors

(MTSC10AC), (MTSC11AC) and (MTSC12AC) molecules are organic bases, which are easily protonated to cationic forms in acidic medium due to the presence of nitrogen, oxygen and sulphur atoms. It is shown from Fig. 2 that HOMOs frontier orbitals electron density distributions, are principally localized on the nitrogen (N) and sulfur atoms (S) (larger electronic density) indicating that are the preferred sites for the electrophilic attack, thus, the most probably sites upon the protonation for all inhibitors under study. The most preferred protonation sites were identified by performing the proton affinities (PA) by using equation below:

$$PA = E_{protonated} - E_{H_3O^+} - E_{neutral} + E_{H_2O}$$

Where $E_{protonated}$, $E_{neutral}$, $E_{H_3O^+}$, and E_{H_2O} are the total energy of the neutral MTSC10AC), (MTSC11AC) and (MTSC12AC) molecules, the protonated ones, the hydronium ion, and water molecule, respectively. The calculated PAs of the nitrogen in triazole heads yields larger PA for N4 than for N1, N2 and S. As an example, in the event of (MTSC12AC), the PAs are -4.403 eV, -4.068 eV, -1,659 eV and -1.793 eV for N4, N2, N1 and S, respectively. This result was confirmed by calculating the total energy for the protonated system that gives the lowest energy upon protonation at N4 atom (-37549.8583 eV). The quantum chemical parameters of the protonated molecules calculated in aqueous phase are summarized in Table 4.

Table 4. The calculated quantum chemical parameters for MTSC10AC, MTSC11AC and MTSC12AC in the protonated form obtained by using DFT at the B3LYP/6-31+G (d, p) basis set in aqueous phase.

Molecule	E_{HOMO} (eV)	E_{LUMO} (eV)	ΔE (eV)	μ (Debye)	TNC (e)	Vi (cm3/mol)	<α> (ua)
MTSC10AC	-7.556	-2.285	5.271	15.6658	-8.441	220.354	288.11
MTSC11AC	-7.451	-2.363	5.088	17.9880	-8.902	244.298	302.82
MTSC12AC	**-7.265**	**-2.509**	**4.756**	**20.3945**	**-9.363**	**261.060**	**317.47**

Analysis calculated parameters quantum data of protonated inhibitors forms in Table 4 show a higher value of E_{HOMO} for MTSC12AC (-7.265 eV) in comparison to MTSC10AC (-7.556 eV) and MTSC11AC (-7.451 eV) which is in accordance with experimental inhibition efficiencies. E_{exp}(%) increases linearly with E_{HOMO} (Fig. 3a), showing that these inhibitors have a high power of offering electrons to the unoccupied d orbital of the metal.

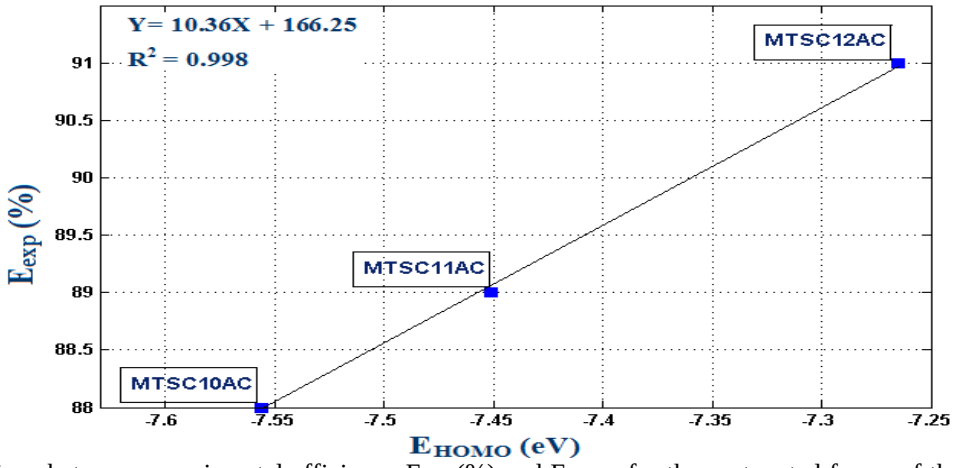

Fig. 3a. Correlations between experimental efficiency E_{exp} (%) and E_{HOMO} for the protonated forms of the inhibitors using B3LYP/6-31G+(d,p).

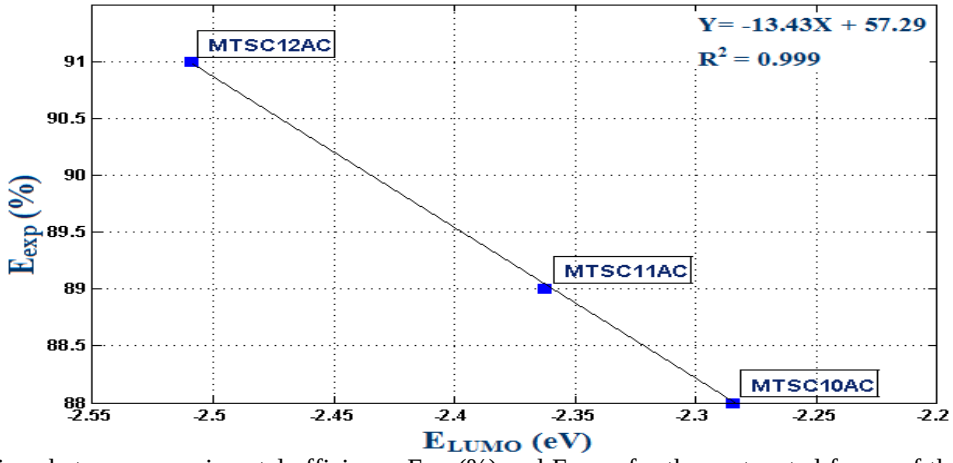

Fig. 3b. Correlations between experimental efficiency E_{exp} (%) and E_{LUMO} for the protonated forms of the inhibitors using B3LYP/6-31G+(d,p).

The E_{LUMO} of this class increases in the order MTSC12AC > MTSC11AC > MTSC10AC, this order is in good agreement with the ranking of inhibition efficiency obtained from the electrochemical polarization method. In addition, Fig. 3b shows that a good correlation was found among E_{LUMO} and E_{exp}(%) for the protonated forms of the molecules, this, proves that these inhibitors can accept electrons from the metal surface. In addition, MTSC12AC has the smallest $\Delta E = E_{LUMO} - E_{HOMO}$ (4.756 eV) compared with the other molecules. Accordingly, one might expect that MTSC12AC molecule has a greater tendencyto adsorb on the metal surface than the other molecules, which is a good agreement with the experimental inhibition efficiency; this is confirmed by Fig. 3c which presents a linear behavior with efficiency. These results are completely different from what we obtained in the case of the neutrals inhibitors. Furthermore, Table 4shown that the dipole moment (μ), total negatives charges (TNC), molecular volume (V_i), and the polarizability <α> of the protonated inhibitors follows the trend MTSC12AC > MTSC11AC > MTSC10AC suggesting that MTSC12AC has the highest inhibition efficiency of the studied molecules, which is in agreement with experimental observations.

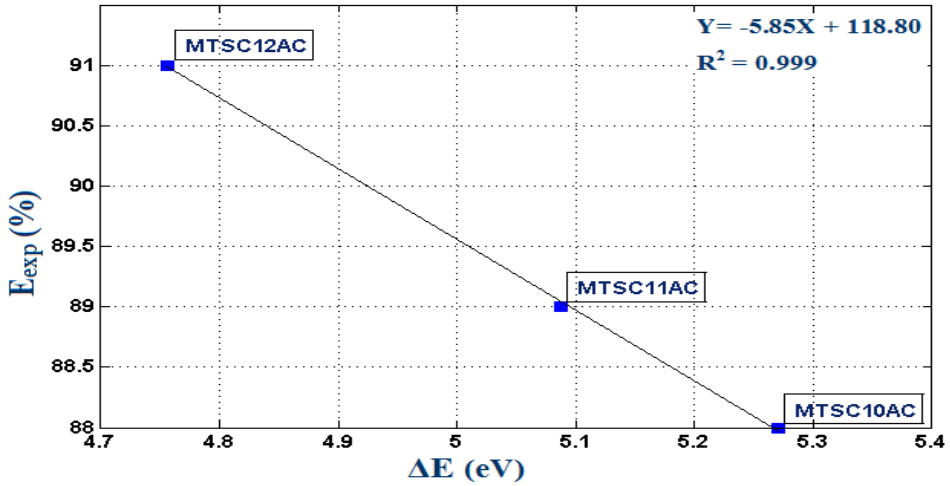

Fig. 3c. Correlations between experimental efficiency E_{exp} (%) and ΔE for the protonated forms of the inhibitors using B3LYP/6-31G+(d,p).

It clearly appears that all the quantum chemical parameters calculated in the protonated form are strongly correlated with experimental inhibition efficiencies. These results show that in acid medium, the protonated form of the inhibitors should make a higher contribution to the corrosion inhibiting effect of the inhibitors on mild steel. In addition, the energies of the highest occupied molecular orbital (HOMO) are clearly correlated with the corrosion inhibition efficiency indicating that, this class of inhibitor molecules can also adsorb on the mild steel surface on the basis of donor–acceptor interactions between π-electrons of the aromatic ring; or else between unshared electron pairs of hetero-atoms and vacant d-orbitals of surface iron atoms. Similarly, the energies of the lowest unoccupied molecular orbital (LUMO) are also strongly correlated with the experimental inhibition efficiency, this could lead to the conclusion that the strongest feedback bonds are formed in the case of the protonated inhibitors increasing the chemical adsorption (chemisorptions) of inhibitor molecules on the steel surface. All inhibitors molecules under study have a similar HOMO and LUMO frontier orbitals electron density distributions, that is why only the contour plots of the Kohn–Sham of HOMO and LUMO of the (MTSC12AC) obtained at the B3LYP/6-31+G(d, p) level in the protonated form were shown in Fig. 4.

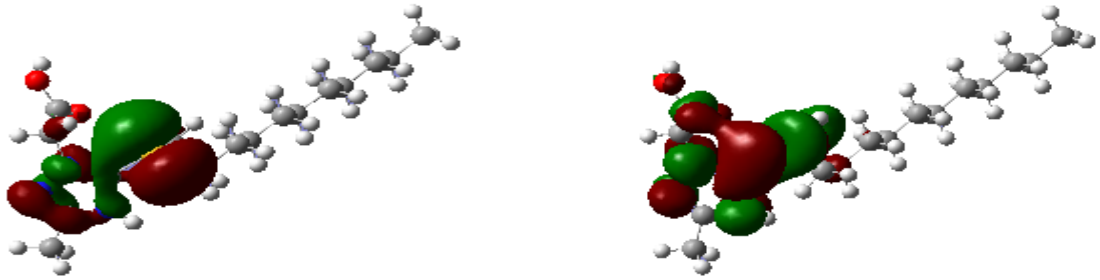

Fig. 4. Contour plots of the Kohn–Sham of HOMO and LUMO of the (MTSC12AC) as obtained at the B3LYP/6-31+G(d, p) level in the protonated form.

From this figure, the amino group of the hydrophilic fragments as well as the thione group has larger HOMOs frontier orbitals electron density distribution, which could make them nucleophilic centers when interacting with metallic surfaces. Mutually, the LUMOs are mostly located in the thione group attached to the hydrophilic fragments, indicating that the preferred sites through them the inhibitors molecules may accept free electrons from the metal by using their anti-bond orbitals to form stable chelates (feedback bond).

3.4. Linear regression analysis

Quantitative structure–activity relationship (QSAR) analysis [14] has been used to correlate the corrosion inhibition activity of the studied molecules with the molecular structures. In which, multidimensional linear least-square fit regression analysis was performed [30], using MATLAB software [34]. In this regression analysis, the inhibitors concentrations (C_i) and the average of experimental inhibition efficiencies (E_{exp} in %) were correlated with obtained molecular properties in the quantum chemical calculations of the protonated inhibitors (Table 4). Experimental measurements, were used to quantify the theoretical corrosion-inhibition

efficiency (E_{cal} in %). The linear model approximates inhibition efficiency (E_{cal} in %) is given in the equation below:

$$E_{cal} = A_j X_j C_i + A_0$$

Where (E_{cal} in %) is the calculated inhibition efficiency, A_j constants are the linear regression coefficients determined by regression analysis, X_j is a quantum chemical index characteristic of molecule (j) and C_i denotes the experiment's concentration (i). In this regression, for proving that these inhibitors can accept electrons from the metal surface forming what is known as feed-back bonds, only the quantum chemical parameters E_{HOMO} and E_{LUMO} were taken into account. The molecular properties and C_i ranging from 10^{-3} to 10^{-5} M, and the below equation was obtained:

$$E_{cal}\ (\%) = (2318.3\ E_{HOMO}) - (8473.6\ E_{LUMO}) + 86.60$$

Fig. 5 shows the correlation between the experimental inhibition efficiency (E_{exp} in %) and the calculated inhibition efficiency (E_{cal} in %). It can be seen from this figure that the model illustrate good correlation with (E_{exp} in %) and (E_{cal} in %), this is justified by every acceptable correlation coefficient (R^2 =0.914) between the calculated and experimental efficiencies. Furthermore, the positive sign of the coefficient of E_{HOMO} can be concluded that the adsorption of these inhibitors on the steel surface it may be chemical mechanism. However, the negative sign of the coefficient of E_{LUMO} could indicate that the π* orbital can also accept the electrons from the metal surface and consequently, the strongest feedback bonds are formed [20]. Both factors may provide proof that the adsorption of these protonated inhibitors on the steel surface is chemical adsorption (chemisorption).

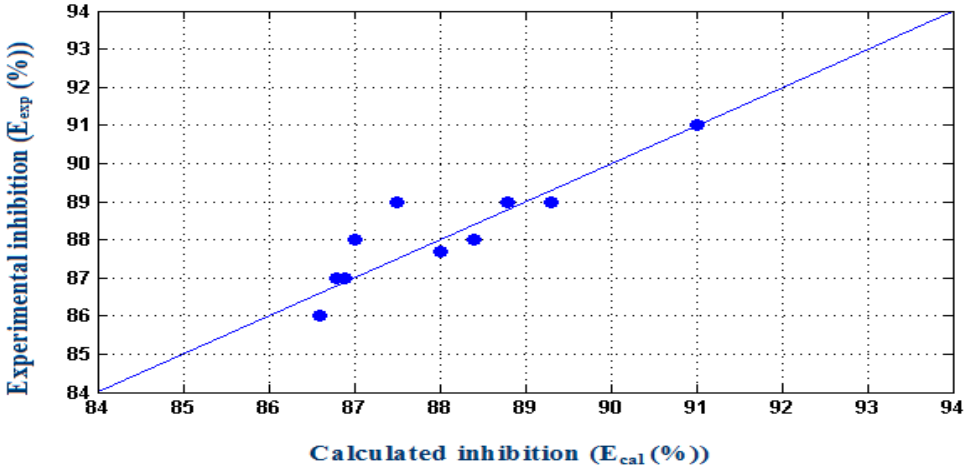

Fig. 5. Experimental inhibitor efficiencies of the protonated inhibitors molecules measured at different concentrations as compared to calculated values from B3LYP/6-31G+(d,p) calculations.

Conclusion

The corrosion-inhibition efficiency of the 3-methyl-1,2,4-triazole-5-thione derivatives as inhibitors for mild steel corrosion in acid medium have been investigated using potentiodynamic and impedance spectroscopy measurements. It has been shown that inhibition efficiency increase with increasing inhibitors concentrations and the hydrocarbon chain length. The MTSC12AC has been selected as the best inhibitor. The molecular properties obtained in the quantum chemical calculations in the protonated form are strongly correlated with experimental inhibition efficiencies, mainly, EHOMO, ELUMO and ΔE. The calculations predict that MTSC12AC is a better corrosion inhibitor than MTSC11AC and MTSC10AC. PCM calculations indicated that polar solvents stabilize the inhibitors molecules by stabilization their frontier molecular orbitals (FMO). A Very acceptable correlation between the calculated and experimental efficiencies were found using linear regression, and feedback bonds formation has been demonstrated, justifying the chemical adsorption.

References

1. AitHaddou B., Chebabe D., Dermaj A., Benassaoui H., El Assyry A., Hajjaji N., Ibn Ahmed S., Srhiri A., *J. Mater. Environ. Sci.*, 7 (2016) 2191.
2. Verma Chandrabhan, Quraishi M.A., Ebenso E.E., Obot I.B., El Assyry A., *J. Mol. Liq.*, 219 (2016) 647.
3. El Assyry A., Benali B., Lakhrissi B., El Faydy M., Ebn Touhami M., Touir R., Touil M., *Res. Chem. Intermed.*, 41 (2015) 3419.
4. Benhiba F., ELaoufir Y., Belayachi M., Zarrok H., El Assyry A., Zarrouk A., Hammouti B., Ebenso E.E., Guenbour A., Al Deyab S.S., Oudda H., *Der Pharm. Lett.*, 6 (2014) 306.

5. Larouj M., ELaoufir Y., Serrar H., El Assyry A., Galai M., Zarrouk A., Hammouti B., Guenbour A., El Midaoui A., Boukhriss S., Ebn Touhami M., Oudda H., *Der Pharm. Lett.*,6 (2014) 324.
6. Ben Hmamou D., Salghi R., Zarrouk A., Zarrok H., Touzani R., Hammouti B., El Assyry A., *J. Environ. Chem. Eng.*, 3 (2015) 2031.
7. Belayachi M., Serrar H., El Assyry A., Oudda H., Boukhris S., Ebn Touhami M., Zarrouk A., Hammouti B., Ebenso Eno E., El Midaoui A., *Int. J. Electrochem. Sci.*, 10 (2015) 3038.
8. ELouadi Y., Abrigach F., Bouyanzer A., Touzani R., Riant O., El Mahi B., El Assyry A., Radi S., Zarrouk A. and Hammouti B., *Der Pharm. Chem.*, 7(8) (2015) 265.
9. Chebabe D., Ait Chikh Z., Dermaj A., Rhattas K., Jazouli T., Hajjaji N., El Mdari F. and Srhiri A., *Corros. Sci.*, 46/11 (2004) 2701.
10. Chebabe D., Dermaj A., Ait chikh Z., Hajjaji N., Srhiri A., *Phys. Chem. News*, 19 (2004) 120.
11. El Hezzat M., Assouag M., Zarrok H., Benzekri Z., El Assyry A., Boukhris S., Souizi A., Galai M., Touir R., Ebn Touhami M., Oudda H. and Zarrouk A., *Der Pharm. Chem.*, 7(10) (2015) 77.
12. (a) Becke A. D., *J. Chem. Phys*. 98 (1993) 5648 (b) Lee C., Yang W., Parr R. G., *Phys. Rev. B.* 37 (1988) 785.
13. Frisch M.J., Trucks G.W., Schlegel H.B., Scuseria G.E., Robb M.A., Cheeseman J.R., Montgomery J.A., Vreven T., Kudin K.N., Burant J.C., Millam J.M., Iyengar S.S., Tomasi J., Barone V., Mennucci B., Cossi M., Scalmani G., Rega N., Petersson G.A., Nakatsuji H., Hada M., Ehara M., Toyota K., Fukuda R., Hasegawa J., Ishida M., Nakajima T., Honda Y., Kitao O., Nakai H., Klene M., Li X., Knox J.E., Hratchian H.P., Cross J.B., Bakken V., Adamo C., Jaramillo J., Gomperts R., Stratmann R.E., Yazyev O., Austin A.J., Cammi R., Pomelli C., Ochterski J.W., Ayala P.Y., Morokuma K., Voth G.A., Salvador P., Dannenberg J.J., Zakrzewski V.G., Dapprich S., Daniels A.D., Strain M.C., Farkas O., Malick D.K., Rabuck A.D., Raghavachari K., Foresman J.B., Ortiz J.V., Cui Q., Baboul A.G., Clifford S., Cioslowski J., Stefanov B.B., Liu G., Liashenko A., Piskorz P., Komaromi I., Martin R.L., Fox D.J., Keith T., Laham A.M.A., Peng C.Y., Nanayakkara A., Challacombe M., Gill P.M.W., Johnson B., Chen W., Wong M.W., Gonzalez C., Pople J.A., Gaussian 09, Revision A02, Gaussian Inc, Wallingford CT, (2009).
14. Hansch C., Leo A., Substituent Constants for Correlation Analysis in Chemistry and Biology; John Wiley and Sons: New York, 1979.
15. Chebabe D., Dermaj A., Ait Chikh Z., Hajjaji N., Rico-Lattes I., Lattes A., *Synth. Commun.*, 34 (2004) 4189
16. (a) Miertius S., Scrocco E., Tomasi J., *Chem. Phys*., 55 (1981) 117 (b) Cancers E., Mennuci B., Tomasi J., *J. Chem. Phys*., 107 (1997) 3032.
17. AitHaddou B., Chebabe D., Dermaj A., Moustafa D., Rhattass K., Hajjaji N., Ibn Ahmed S., Srhiri A., *International Journal Of Scientific & Engineering Research*, 7 (7) (2016) 588.
18. Ashassi-Sorkhabi H., Shabani B., Aligholipour B., Seifzadeh D., *Appl. Surf.Sci*., 252 (2006) 4039.
19. Gece G., Bilgic S., *Corros. Sci*., 51 (2009) 1876.
20. Khalil N., *Electrochim. Acta*., 48 (2003) 2635.
21. Fang J., Li J., *J. Mol. Struct. (THEOCHEM)*, 593 (2002) 179.
22. Zhou Z., Parr R.G., *J. Am. Chem. Soc.*, 112 (1990) 5720.
23. Gökhan Gece, *Corros. Sci.*, 50 (2008) 2981.
24. Dwivedi A., Misra N., *Der Pharma Chemica*, 2. 2 (2010) 58.
25. Li X., Deng S., Fu H., Li T., *Electrochim. Acta*., 54 (2009) 4089.
26. Kandemirli F., Hoscan M., Dimoglo A., Esen S., *Phosphorus Sulfur Silicon Relat. Elem.*, 183 (2008) 1954.
27. Uwe Hohm, *J. Phys. Chem. A*, 104 (36) (2000) 8418.
28. Taner Arslan, Kandemirli F., Ebenso Eno E., Ian Love, Hailemichael Alemu, *Corros. Sci.*, 51 (2009) 35.
29. Masouda M.S., Awad M.K., Shaker M.A., El-Tahawy M.M.T., *Corros. Sci.*, 52 (2010) 2387.
30. Touil M., Hajjaji N., Sundholm D., Rabaâ H., *Int. J. Quantum. Chem*. 113 (2013)1365.
31. EL Aoufir Y., Lgaz H., Bourazmi H., Kerroum Y., Ramli Y., Guenbour A., Salghi R., El-Hajjaji F., Hammouti B., Oudda H., *J. Mater. Environ. Sci.* 7 (12) (2016) 4330-4347
32. Tomasi J., Mennucci B., Cammi R.,*Chem. Rev*., 105 (2005) 2999.
33. Mennucci B., *J. Phys. Chem. Lett*., 1 (2010) 1666.
34. Sorensen D. C., Lehoucq R. B., Yang C., Maschhoff K., ARPACK, Copyright (2001), Rice University.